

两个含双膦配体和[2,3-*f*]吡嗪并[1,10]菲咯啉的 Cu(I)配合物的合成、结构及光谱学性质

卢延磊¹ 朱 宁¹ 赵宇萌¹ 林 森¹ 匡晓楠¹
李中峰¹ 辛秀兰² 杨玉平³ 金琼花^{*,1} 张江威^{*,4}

(¹ 首都师范大学化学系, 北京 100048)

(² 北京工商大学食品学院, 北京 100048)

(³ 中央民族大学理学院, 北京 100081)

(⁴ 中国科学院大连化学物理研究所催化基础国家重点实验室金催化中心, 大连 116023)

摘要: 合成了 2 个新的铜(I)配合物, [Cu(dppBz)(dpq)]ClO₄ (**1**)和[Cu(dppe)(dpq)]ClO₄ (**2**)(dppBz=1,2-双(二苯基膦)苯, dppe=1,2-双(二苯基膦)乙烷, dpq=[2,3-*f*]吡嗪并[1,10]菲咯啉),通过 X 射线单晶衍射分析、元素分析、红外光谱、紫外吸收光谱、荧光光谱、核磁共振光谱和太赫兹时域光谱对其进行了分析和表征。**1** 的中心 Cu(I)离子通过二亚胺配体和双膦配体共同螯合形成变形四面体结构,**2** 的结构与 **1** 类似。配合物 **2** 的发光光谱表明它的发光具有金属-配体电荷转移(MLCT)特性。对配合物 **1** 和 **2** 在 0.2~2.8 THz 范围内进行了太赫兹时域光谱分析,结果表明 0.40~0.90 THz 的吸收与中心 Cu(I)离子的配位有关。

关键词: [2,3-*f*]吡嗪并[1,10]菲咯啉;铜(I)配合物;荧光;太赫兹时域光谱

中图分类号: O614.121

文献标识码: A

文章编号: 1001-4861(2019)04-0720-09

DOI: 10.11862/CJIC.2019.059

Syntheses, Structural Characterizations and Spectroscopic Properties of Two Copper(I) Complexes Based on Diphosphine Ligands and [2,3-*f*]pyrazino[1,10]phenanthroline

LU Yan-Lei¹ ZHU Ning¹ ZHAO Yu-Meng¹ LIN Sen¹ KUANG Xiao-Nan¹ LI Zhong-Feng¹

XIN Xiu-Lan² YANG Yu-Ping³ JIN Qiong-Hua^{*,1} ZHANG Jiang-Wei^{*,4}

(¹Department of Chemistry, Capital Normal University, Beijing 100048, China)

(²School of Food and Chemical Engineering, Beijing Technology and Business University, Beijing 100048, China)

(³School of Science, Minzu University of China, Beijing 100081, China)

(⁴State Key Laboratory of Catalysis & Gold Catalysis Research Center, Dalian Institute of
Chemical Physics, Chinese Academy of Sciences, Dalian, Liaoning 116023, China)

Abstract: Two novel copper(I) complexes [Cu(dppBz)(dpq)]ClO₄ (**1**) and [Cu(dppe)(dpq)]ClO₄ (**2**) (dppBz=1,2-bis(diphenylphosphino)benzene, dppe=1,2-bis(diphenylphosphino)ethene, dpq=[2,3-*f*]pyrazino[1,10]phenanthroline) have been synthesized and characterized by X-ray diffraction, elemental analysis, infrared spectroscopy, absorption spectra, luminescent spectra, ¹H NMR, ³¹P NMR spectroscopy and terahertz (THz) time-domain absorption spectroscopy. The central Cu(I) ion is chelated by a diimine ligand and a diphosphine ligand forming a distorted tetrahedron configuration for **1**, and the configuration of **2** is similar to **1**. The luminescent spectra of **2** indicated

收稿日期: 2018-11-19。收修改稿日期: 2018-12-19。

国家自然科学基金(No.81573822, 11574408, 21171119, 21376008, 21701168),北京市自然科学基金(No.2172017)和辽宁省自然科学基金(No.20170540897)资助项目。

*通信联系人。E-mail: jinqh@cnu.edu.cn, jwzhang@dicp.ac.cn; 会员登记号: S06N3669M1105。

that the emission has metal-to-ligand charge transfer (MLCT) characteristics. The terahertz time-domain absorption spectroscopy analysis in a range of 0.2~2.8 THz showed that the absorption peaks at 0.40~0.90 THz are related to the coordination of the central Cu(I). CCDC: 1874580, **1**; 1874581, **2**.

Keywords: [2,3-*f*]pyrazino[1,10]phenanthroline; Cu(I) complexes; fluorescence; terahertz (THz) time-domain absorption spectroscopy

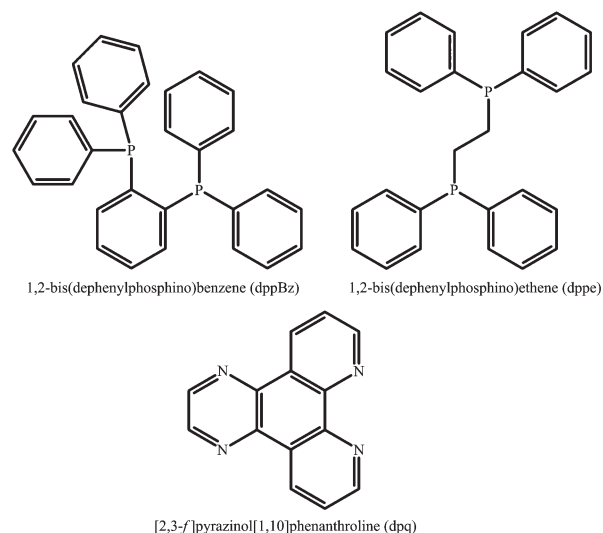
0 Introduction

Currently, there are plentiful scientific researches in luminescent metal complexes used in climate science, materials science. The Cu(I) complexes^[1-10] are extensively studied due to the high relative abundance and environmental friendliness of copper^[5,11-13] in comparison to some precious metals, such as Os, Pt, Ir^[14-15]. Especially heteroleptic Cu(I) complexes, such as copper(I)-diimine-phosphine complexes^[16-18], attract wide interest in recent years.

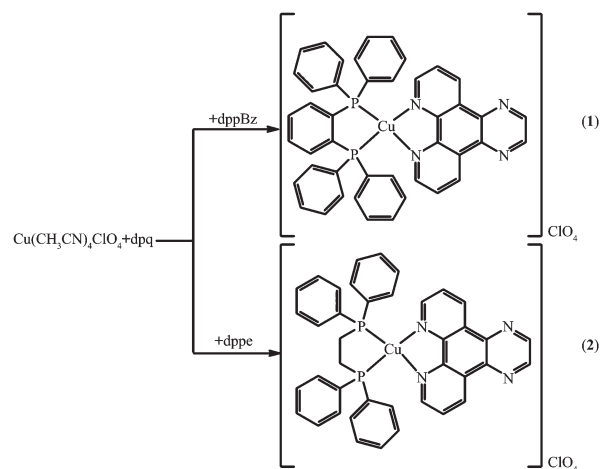
1,10-phenanthroline(1,10-phen), on account of its peculiar conjugacy of heteroaromatic, can easily coordinate with metal ion forming stable metal complexes^[19]. 1,10-phen and its derivatives with unique rigidity structures often show metal-to-ligand charge transfer (MLCT) characteristics owing to the lower π^* orbital energy. In addition, they are also optically active ligands used to synthesize luminescent complexes^[20].

Following the earlier studies on heteroleptic copper(I) complexes bearing 1,10-phen derivatives and diphosphine ligands^[18,21], we chose [2,3-*f*]pyrazino[1,10]phenanthroline (dpq) as diimine ligand, 1,2-bis(diphenylphosphino)benzene (dppBz) and 1,2-bis(diphenylphosphino)ethane (dppe) as diphosphine ligands (Scheme 1) to prepare two new complexes. The relevant synthesis routes are summarized in Scheme 2. We describe herein the synthesis, structure characterization and spectroscopic properties of the two new Cu(I) complexes with dpq ligand [Cu(dppBz)(dpq)]ClO₄ (**1**) and [Cu(dppe)(dpq)]ClO₄ (**2**) (Scheme 2). Complexes **1** and **2** have been isolated and characterized by X-ray diffraction, elemental analysis, infrared spectroscopy, absorption spectra, ¹H NMR and ³¹P NMR spectroscopy, terahertz (THz) time-domain absorption spectroscopy, and emission property of **2** is also studied. Single-crystal X-ray diffraction analysis

reveals that a 1D hollow tube-like structure is formed by C-H $\cdots\pi$ intermolecular forces and hydrogen bonds in complex **1**, while two units are linked together via one π - π stacking force and two C-H $\cdots\pi$ intermolecular forces in complex **2**. The terahertz spectra of the two complexes were measured by the ultrashort pulses of coherent terahertz radiation (0.1~4 THz, 3~133 cm⁻¹). Terahertz spectra is a vibrational spectroscopy that is used to probe the vibrational



Scheme 1 Chemical structures of ligands dppBz, dppe and dpq



Scheme 2 Synthetic routes for complexes **1** and **2**

modes in the far-infrared and sub-millimeter region of the electro-magnetic spectrum, which is pretty useful in characterizing the structures and studying the functions of polarity complexes^[22].

1 Experimental

1.1 Materials and measurements

All commercially available starting materials were used as received, and solvents were used without any purification. FT-IR spectra (KBr pellets) were measured on a Perkin-Elmer Infrared spectrometer. Room-temperature fluorescence spectra were measured on F-4500 FL Spectrophotometer. C, H and N elemental analysis were carried out on an Elementar Vario MICRO CUBE (Germany) elemental analyzer. ¹H NMR and ³¹P NMR were recorded at room temperature with a Bruker DPX 600 spectrometer. The THz absorption spectra were recorded on the THz time domain device of Minzu University of China, based on photoconductive switches for generation and electro-optical crystal detection of the far-infrared light, effective frequency in a range of 0.2~2.8 THz^[23-24].

1.2 Synthesis of [Cu(dppBz)(dpq)]ClO₄ (1)

Complex **1** was prepared by the reaction of [Cu(CH₃CN)₄]ClO₄ (0.065 4 g, 0.2 mmol), dppBz (0.089 3 g, 0.2 mmol) and dpq (0.046 4 g, 0.2 mmol) in the mixed solvents of 5 mL CH₂Cl₂ and 5 mL CH₃OH. The mixture was stirred for 6 hours and filtered. Yellowish crystals were obtained from the filtrate after standing at room temperature for 4~5 days. Yield: 67%. Element analysis Calcd. for C₄₄H₃₂CuN₄P₂ClO₄(%): C, 62.78; H, 3.83; N, 6.66. Found (%): C, 62.54; H, 3.80; N, 6.54. IR data (cm⁻¹, KBr pellets): 2 918w, 1 632m, 1 436m, 1 402m, 1 385m, 1 121s, 1 094vs, 814w, 736m, 695m, 622w, 521m, 440w. ¹H NMR (600 MHz, DMSO-d₆, 298 K): δ 7.26~7.76 (m, CH_{benzene} from dppBz), 8.06~9.55 (m, heterocyclic hydrogen from dpq, including solvent signals); ³¹P NMR (600 MHz, DMSO-d₆, 298 K): δ -3.53

(s, phosphorus from dppBz).

1.3 Synthesis of [Cu(dppe)(dpq)]ClO₄ (2)

Complex **2** was prepared in a manner similar to the described for **1** except that dppe (0.079 7 g, 0.2 mmol) was used instead of dppBz. Orange-red crystals of **2** were obtained from the filtrate after standing at the room temperature for several weeks. Yield: 63%. Element analysis Calcd. for C₄₀H₃₂CuN₄P₂ClO₄(%): C, 60.53; H, 4.06; N, 7.06. Found(%): C, 60.37; H, 4.07; N, 6.87. IR data (cm⁻¹, KBr pellets): 1 628m, 1 435m, 1 403m, 1 386m, 1 121s, 1 094vs, 815w, 738m, 698m, 623w, 520m, 440w. ¹H NMR (600 MHz, DMSO-d₆, 298 K): δ 7.37~7.47 (m, CH_{benzene} from dppe), 8.17~9.63 (m, heterocyclic hydrogen from dpq, including solvent signals); ³¹P NMR (600 MHz, DMSO-d₆, 298 K): δ -3.53 (s, phosphorus from dppe).

1.4 Structure determination

Single crystals of the title complexes were mounted on a Bruker Smart 1000 CCD diffractometer equipped with a graphite-monochromated Mo Kα (λ=0.071 073 nm) radiation at 298(2) K. Semi-empirical absorption corrections were applied using SABABS program^[25]. All the structures were solved by direct methods using SHELXS program of the SHELXTL-97 package and refined with SHELXL-97^[26-27]. Metal atom centers were located from the E-maps and other non-hydrogen atoms were located in successive difference Fourier syntheses. The final refinements were performed by full matrix least-squares methods with anisotropic thermal parameters for non-hydrogen atoms on *F*². The hydrogen atoms were generated geometrically and refined with displacement parameters riding on the concerned atoms.

Crystallographic data and experimental details for structural analysis are summarized in Table 1, and selected bond lengths and angles of complexes **1**~**2** are summarized in Table 2.

CCDC: 1874580, **1**; 1874581, **2**.

Table 1 Crystallographic data for complexes **1** and **2**

	1	2
Formula	C ₈₉ H ₆₈ Cl ₂ Cu ₂ N ₆ O ₁₂ P ₄	C ₄₀ H ₃₂ CuN ₄ P ₂ ClO ₄
Formula weight	1 735.35	793.62
Crystal system	Triclinic	Monoclinic

Continued Table 1

Space group	$P\bar{1}$	$C2/c$
Crystal size / mm	0.40×0.18×0.02	0.40×0.32×0.30
a / nm	0.977 9(2)	1.346 81(11)
b / nm	1.674 5(3)	2.419 7(2)
c / nm	2.511 5(5)	2.664 0(2)
α / (°)	78.66(3)	
β / (°)	79.53(3)	103.034(2)
γ / (°)	75.84(3)	
V / nm ³	3.871 1(15)	8.458(12)
Z	2	8
D_c / (g·cm ⁻³)	1.484	1.246
$F(000)$	1 776	3 264
Goodness-of-fit on F^2	1.034	1.039
R_{int}	0.043 1	0.096 3
$R_1 [I > 2\sigma(I)]^a$	0.067 7	0.064 6
$wR_2 [I > 2\sigma(I)]^b$	0.149 9	0.098 6
R_1 (all data) ^a	0.093 3	0.139 5
wR_2 (all data) ^b	0.165 5	0.106 8

^a $R_1 = \sum (|F_o| - |F_c|) / \sum |F_o|$; ^b $wR_2 = [\sum w(|F_o|^2 - |F_c|^2)^2 / \sum w(F_o^2)]^{1/2}$.

Table 2 Selected bond lengths (nm) and bond angles (°) for complexes **1** and **2**

1					
Cu(1)-P(1)	0.226 29(15)	Cu(1)-P(2)	0.239(15)	Cu(1)-N(1)	0.202 5(4)
Cu(1)-N(2)	0.207 7(4)	Cu(2)-P(3)	0.220 11(14)	Cu(2)-P(4)	0.251 0(15)
Cu(2)-N(5)	0.200 3(4)	Cu(2)-N(6)	0.206 4(4)		
P(1)-Cu(1)-P(2)	89.95(6)	N(2)-Cu(1)-P(1)	109.55(12)	N(2)-Cu(1)-P(2)	123.07(12)
N(2)-Cu(1)-N(1)	81.76(16)	N(1)-Cu(1)-P(1)	128.60(12)	N(1)-Cu(1)-P(2)	123.53(12)
P(4)-Cu(2)-P(3)	91.99(5)	N(5)-Cu(2)-P(3)	133.78(12)	N(5)-Cu(2)-P(4)	122.71(12)
N(6)-Cu(2)-P(3)	118.71(11)	N(6)-Cu(2)-P(4)	107.14(11)	N(6)-Cu(2)-N(5)	81.97(15)
2					
Cu(1)-N(2)	0.204 2(3)	Cu(1)-N(1)	0.207 6(3)	Cu(1)-P(1)	0.226 88(14)
Cu(1)-P(2)	0.227 53(14)				
N(2)-Cu(1)-N(1)	80.83(15)	N(2)-Cu(1)-P(1)	115.80(11)	N(1)-Cu(1)-P(1)	124.75(11)
N(2)-Cu(1)-P(2)	129.43(11)	N(1)-Cu(1)-P(2)	119.13(11)	P(1)-Cu(1)-P(2)	91.22(5)

2 Results and discussion

2.1 Infrared spectroscopy and NMR spectra

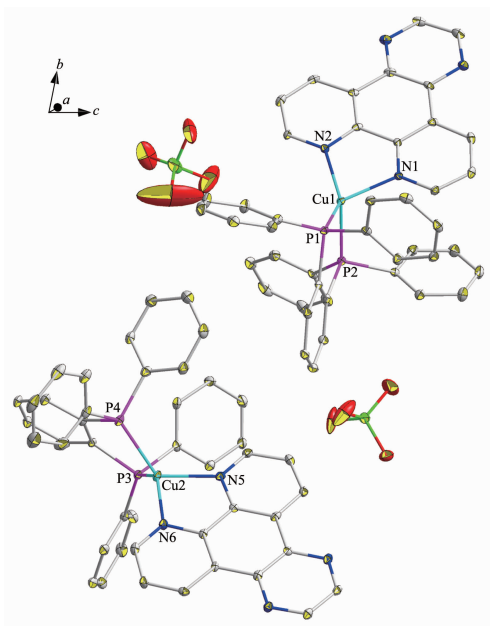
The infrared spectra of complexes **1** and **2** showed that the absorption peaks around 1 436~1 386 cm⁻¹ are put down to C-C absorbing vibration of the phenyl rings in diphosphine ligands, and the middle absorption peaks around 1 350 cm⁻¹ are due to

C-H bending vibration in diimine ligands. In addition to the absorption of chemical bonds on the cation skeleton, there were also characteristic absorption peaks of counter ions, such as the absorption of the Cl-O stretch vibration around 1 093 cm⁻¹ [28].

2.2 Description of crystal structures

Complex **1** is a dimer composed of one asymmetric unit containing two [Cu(dppBz)(dpq)]ClO₄.

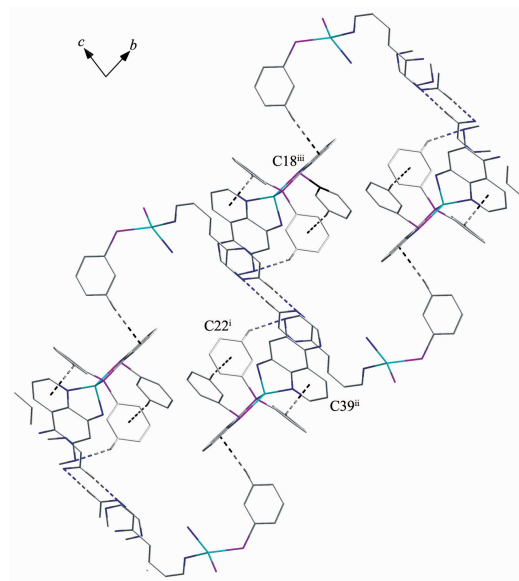
Single-crystal X-ray diffraction analysis reveals that complex **1** crystallizes in triclinic system with $P\bar{1}$ space group. The molecular structure is shown in Fig.1. Selected bond distances and bond angles for complex are shown in Table 2. Each Cu(I) ion is four-coordinated and attach to four atoms (two atoms are from chelating dppBz ligand and the other two are from chelating dpq ligand), forming the cation $[\text{Cu}(\text{dppBz})(\text{dpq})]^+$, while the ClO_4^- anion plays the role of balancing the charge. The geometry around each Cu(I) center is distorted tetrahedral configuration because the angles in a range of $81.97(15)^\circ \sim 133.78(12)^\circ$. The bonds Cu-N (P) in a range of $0.200\ 3\ (4) \sim 0.262\ 9(15)$ nm are close to those in analogous complexes^[29-30]. Single X-ray diffraction reveals that $[\text{Cu}(\text{dppBz})(\text{dpq})]^+$ units form a 1D hollow tube-like structure through two hydrogen bonds: $\text{C}(23) \cdots \text{H}(23) \cdots \text{N}(3)$ ($\text{C}(23) \cdots \text{N}(3)$



All hydrogen atoms are omitted for clarity; Thermal ellipsoids are drawn at the 30% probability level

Fig.1 Molecular structure of complex **1**

$0.253\ \text{nm}$) and $\text{C}(88) \cdots \text{H}(88) \cdots \text{N}(7)$ ($\text{C}(88) \cdots \text{N}(7)$ $0.260\ \text{nm}$), as well as three $\text{C}-\text{H} \cdots \pi$ interactions. Just like in the reported complexes^[31], $\text{C}-\text{H} \cdots \pi$ interactions play a critical role in structural orientation (Fig.2, Table 3).



Most of hydrogen atoms, all anions and a part of phenyl rings are omitted for clarity; Symmetry codes: ⁱ $x, -1+y, -1+z$; ⁱⁱ $x, -1+y, -1+z$; ⁱⁱⁱ $1-x, 1-y, -z$

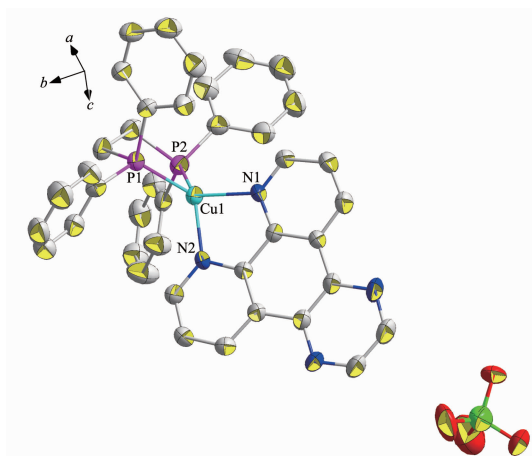
Fig.2 One-dimensional infinite chain of complex **1**

Single-crystal X-ray diffraction analysis reveals that complex **2** crystallizes in monoclinic system with space group $C2/c$. As shown in Fig.3, it can be seen that the two N atoms of dpq ligand and two P atoms of dppe ligand chelate to Cu(I), forming a mononuclear complex bearing a distorted tetrahedral configuration centered on copper(I). In complex **2**, the average bond distances of Cu-P(N) is $0.216\ 6\ \text{nm}$, which is larger than that in the reported complexes bearing dppe ligand^[32]. Two neighboring molecules in complex **2** are connected together by $\pi \cdots \pi$ stacking ($0.395\ \text{nm}$) and $\text{C}-\text{H} \cdots \pi$ interactions (Fig.4, Table 3).

Table 3 Intermolecular $\text{C}-\text{H} \cdots \pi$ interactions in complexes **1** and **2**

	C-H \cdots ring (<i>i</i>)	$d(\text{H} \cdots \text{R}) / \text{nm}$	$\angle \text{C}-\text{H} \cdots \text{R} / (^\circ)$	$d(\text{C} \cdots \text{R}) / \text{nm}$
1	$\text{C}(5)-\text{H}(5) \rightarrow \text{R}(1)^{\text{i}}$	0.284	166	0.374 62
	$\text{C}(27)-\text{H}(27) \rightarrow \text{R}(2)^{\text{ii}}$	0.272	123	0.332 48
	$\text{C}(75)-\text{H}(75) \rightarrow \text{R}(3)^{\text{iii}}$	0.289	156	0.376 41
2	$\text{C}(20)-\text{H}(20) \rightarrow \text{R}(4)^{\text{iv}}$	0.280	140	0.355 72

$\text{R}(1)=\text{C}(19) \sim \text{C}(24)$, $\text{R}(2)=\text{N}(2)$, $\text{C}(36) \sim \text{C}(40)$, $\text{R}(3)=\text{C}(13) \sim \text{C}(18)$, $\text{R}(4)=\text{C}(29) \sim \text{C}(34)$; Symmetry codes: ⁱ $x, -1+y, -1+z$; ⁱⁱ $x, -1+y, -1+z$; ⁱⁱⁱ $1-x, 1-y, -z$; ^{iv} $1.5-x, 0.5-y, 1-z$

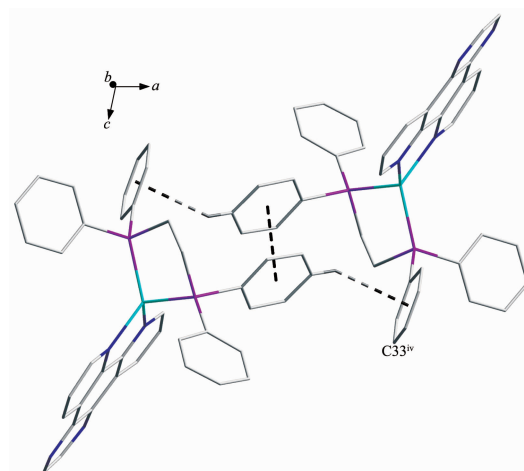


All hydrogen atoms are omitted for clarity; Thermal ellipsoids drawn at the 30% probability level

Fig.3 Molecular structure of complex **2**

2.3 Fluorescence spectra

At room temperature, the solid-state excitation and emission spectra of complex **1** and **2** were measured (Fig.5). We cannot get the excitation and emission data of complex **1**. The photophysical parameters of complex **2** are summarized in Table 4. The ligand dppe exhibited fluorescence signal at 434 nm with an excitation maximum at 310 nm^[33-34]. Complex **2** exhibited yellow-orange light emission when it was excited with UV light, and the emission maxima at 298 K was



Most of hydrogen atoms are omitted for clarity; Symmetry codes: ^{iv} 1.5-x, 0.5-y, 1-z

Fig.4 Two neighboring molecules in complex **2** connected together by $\pi \cdots \pi$ stacking and C-H $\cdots\pi$ interactions

observed at 563 nm with $\lambda_{\text{max}}=366$ nm. The fluorescence spectrum at 298 K was broad without vibronic progressions, indicating that the excited state of the emission has a charge-transfer characteristic at ambient temperature^[35]. According to the analysis of the absorption spectrum (2.4 Absorption spectra), the luminescence is attributed to metal-to-ligand charge transfer.

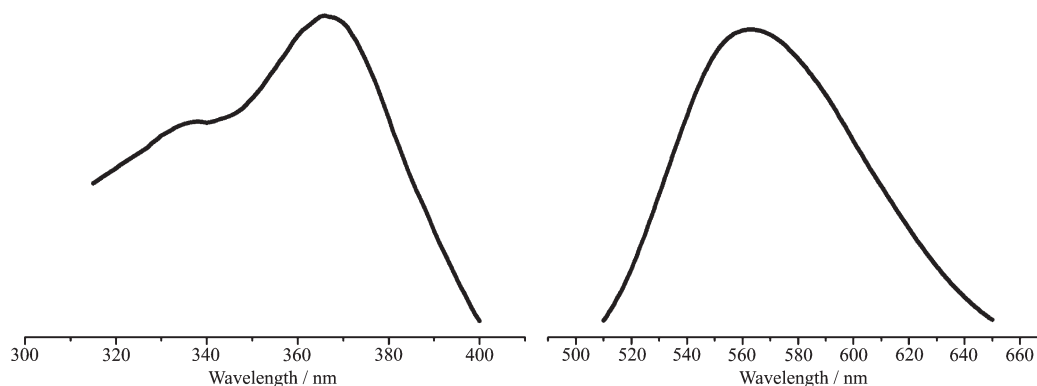


Fig.5 Solid-state excitation (left) and emission (right) spectra of complex **2** at 298 K

Table 4 Luminescence properties of complex **2** in solid state at 298 K

	λ_{max}^a / nm	τ_{av}^b / μs	Φ^c	k_r^d / s^{-1}	k_{nr}^e / s^{-1}
2	563	4.8	0.12	2.50×10^4	1.83×10^5

^a Emission maximum; ^b Average emission lifetime; ^c Photoluminescence quantum yield in the solid state; ^d Radiative rate constant k_r was estimated by Φ/τ_{av} ; ^e Non-radiative rate constant k_{nr} was estimated by $(1-\Phi)/\tau_{\text{av}}$

2.4 Absorption spectra

Absorption spectra of complexes **1** and **2** were

obtained (Fig.6), in spite of that the fluorescence data of complex **1** were not gained. From the absorption

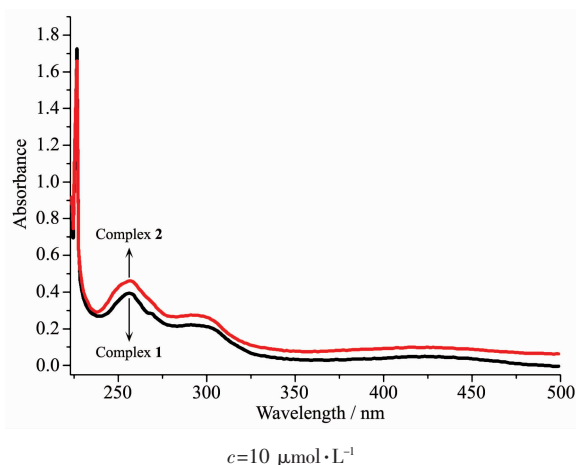


Fig.6 Absorption spectra of complexes **1** and **2** in CH_2Cl_2

spectra, the following conclusions can be drawn. On the one hand, the complexes had strong UV absorption peaks in a range of 280 ~290 nm. The absorption peaks in this range show the intraligand charge transfer (ILCT) characteristics^[36] of complexes **1** and **2**. On the other hand, low-energy UV absorption peaks around 400 ~450 nm can be attributed to metal-to-ligand charge transfer (MLCT), which are consistent

with reported heteroleptic copper(I) complexes^[37].

2.5 Terahertz (THz) time-domain absorption spectroscopy

The terahertz (THz) time-domain absorption spectra of the diphosphine ligands dppBz, dppe, the diimine ligand dpq and complexes **1**~**2** were measured in a range 0.2 ~2.8 THz (Fig.7 and Fig.8) at room temperature. The relevant data are summarized in Table 5.

The results show that the types of ligands as well as the structures of complexes both have a significant impact on the absorption peaks of the terahertz time-domain absorption spectroscopy. It's worth noting that the newly formed terahertz spectra peaks for the complexes (0.67, 0.73 THz for **1**, and 0.53, 0.67, 0.74, 0.87 THz for **2**) in a range of 0.40 ~0.90 THz are related to the coordination of copper(I). As shown in Fig.7, Fig.8 and Table 5, the terahertz spectra peaks of ligands are shown at 0.27, 0.79, 2.17, 2.43 THz for dppBz, 0.79, 0.93, 1.00, 1.46, 1.67, 1.79, 1.90, 2.40 THz for dppe, and 0.32, 1.00, 1.38, 1.44, 1.70, 1.79,

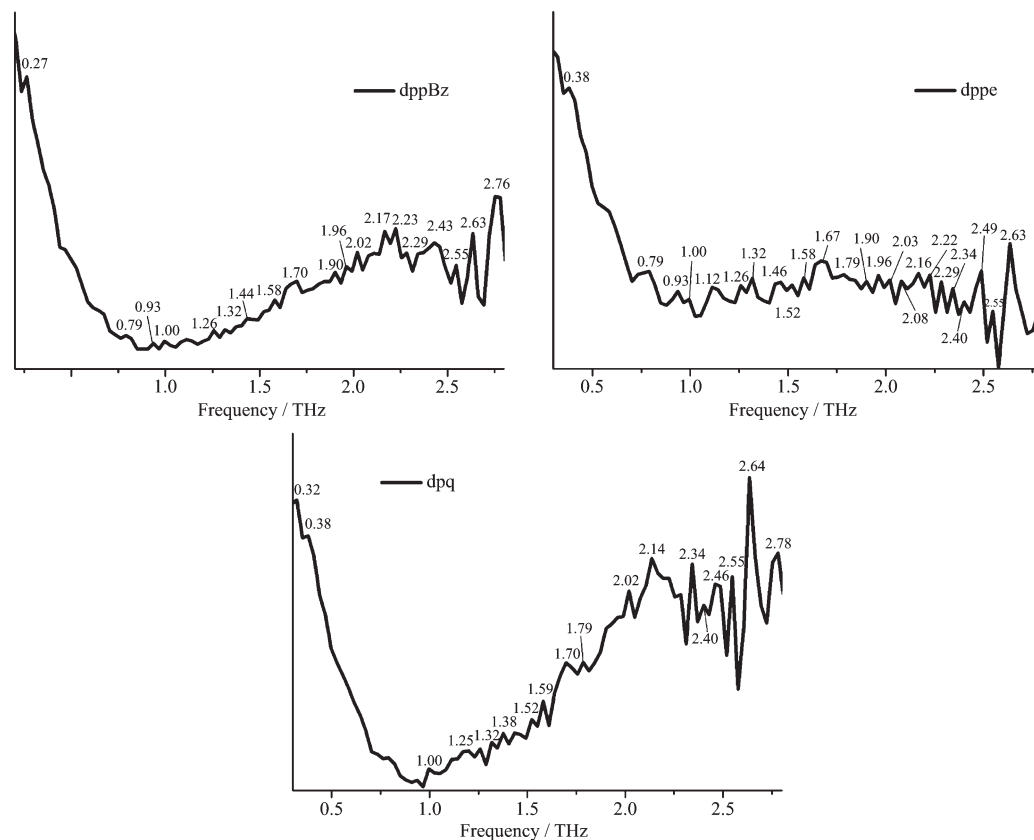
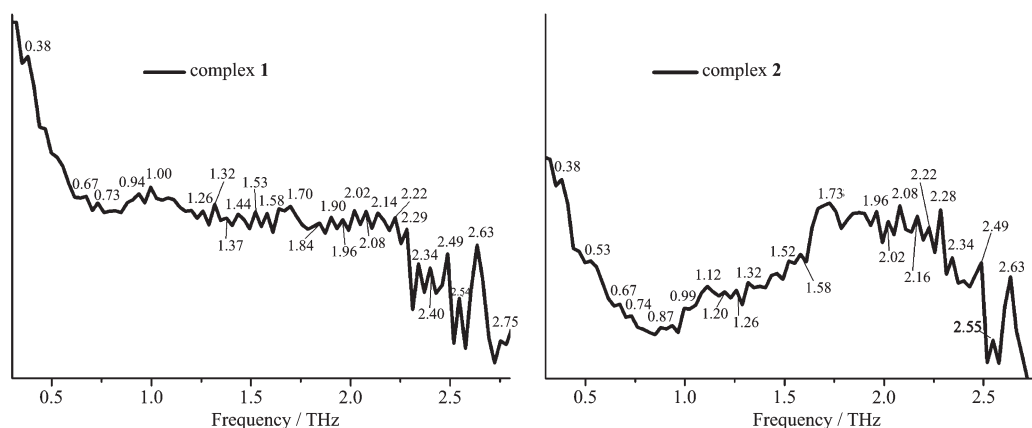


Fig.7 THz absorption spectra of ligands: dppBz, dppe, dpq

Fig.8 THz absorption spectra of complexes **1** and **2**Table 5 Terahertz spectra peaks of the ligands and complexes **1-2**

Compound	Frequency / THz										
dppBz	0.27	0.79	0.93	1.00	1.26	1.32	1.44	1.58	1.70	1.90	1.96
	2.02	2.17	2.23	2.29	2.43	2.55	2.63	2.76			
dppe	0.38	0.79	0.93	1.00	1.12	1.26	1.32	1.46	1.52	1.58	1.67
	1.79	1.90	1.96	2.03	2.08	2.16	2.22	2.29	2.34	2.40	2.49
	2.55	2.63									
dpq	0.32	0.38	1.00	1.25	1.32	1.38	1.44	1.52	1.59	1.70	1.79
	2.02	2.14	2.34	2.40	2.46	2.55	2.64	2.78			
1	0.38	0.67	0.73	0.94	1.00	1.26	1.32	1.37	1.44	1.53	1.58
	1.70	1.84	1.90	1.96	2.02	2.08	2.14	2.22	2.29	2.34	2.40
	2.49	2.54	2.63	2.75							
2	0.38	0.53	0.67	0.74	0.87	0.99	1.12	1.20	1.26	1.32	1.52
	1.58	1.73	1.96	2.02	2.08	2.16	2.22	2.28	2.34	2.49	2.55
	2.63										

2.14, 2.40, 2.46, 2.78 THz for dpq. By comparing the THz absorption spectra of the complexes with those of the ligands, we can note that the peaks of ligands disappeared or moved after reaction. Therefore, terahertz time-domain absorption spectroscopy is a sensitive method for distinguishing and determining the weeny difference in complexes.

3 Conclusions

Two functional heteroleptic Cu (I) complexes containing diphosphine ligands and 1,10-phen derivative [2,3-*f*]pyrazino[1,10]phenanthroline have been synthesized and characterized by X-ray diffraction, elemental analysis, infrared spectroscopy, absorption spectra, NMR spectra, fluorescence spectra, terahertz (THz) time-domain absorption spectroscopy. Single X-ray diffraction reveals that complex **1** is a dimer

composed of one asymmetric unit, containing two [Cu(dppBz)(dpq)]ClO₄, with the unit cells packing into a 1D hollow tube-like structure by hydrogen bonds and C-H $\cdots\pi$ intermolecular forces. Complex **2** is a simple mononuclear structure. Two neighboring molecules of **2** are connected together by $\pi\cdots\pi$ stacking and C-H $\cdots\pi$ interactions. Absorption spectrum reveals that the luminescence of complexes is derived from metal-to-ligand charge transfer (MLCT). Terahertz time-domain absorption spectroscopy can help identify the tiny differences of structures of complexes.

References:

- [1] Yang X, Zhou G, Wong W Y. *Chem. Soc. Rev.*, **2015**,**44**: 8484-8575
- [2] Tsuge K, Chishina Y, Kitamura N, et al. *Coord. Chem. Rev.*,

- 2016,306**:636-651
- [3] Ford P C, Cariati E, Bourassa J. *Chem. Rev.*, **1999,99**:3625-3648
- [4] Luo S P, Mejia E, Beller M, et al. *Angew. Chem. Int. Ed.*, **2013,52**:419-423
- [5] Hayashi T, Kobayashi A, Kato M, et al. *Inorg. Chem.*, **2015,54**:8905-8913
- [6] Perruchas S, Le G, Boilot J P, et al. *J. Am. Chem. Soc.*, **2010,132**:10967-10969
- [7] Chou C C, Su C C, Yeh A. *Inorg. Chem.*, **2005,44**:6122-6128
- [8] Armaroli N, Accorsi G, Welter R, et al. *Adv. Mater.*, **2006,18**:1313-1316
- [9] Wang D, Zhang W, Zhou Y, et al. *Chemistry Select*, **2006,1**:1917-1920
- [10] Costa R D, Ortí E, Armaroli N, et al. *Angew. Chem. Int. Ed.*, **2012,51**:8178-8211
- [11] Czerwieniec R, Leitzl M J, Yersin H, et al. *Coord. Chem. Rev.*, **2016,325**:2-28
- [12] Osawa M, Hoshino M, Yashima M, et al. *Dalton Trans.*, **2015,44**:8369-8378
- [13] Chen J L, Guo Z H, Wang J Y, et al. *Dalton Trans.*, **2016,45**:696-705
- [14] Lamansky S, Djurovich P, Thompson M E, et al. *J. Am. Chem. Soc.*, **2001,123**:4304-4312
- [15] Deason J C, Young R H, Huo S, et al. *Inorg. Chem.*, **2010,49**:9151-9161
- [16] Cuttall D G, Kuang S M, McMillin D R, et al. *J. Am. Chem. Soc.*, **2002,124**:6-7
- [17] Sun Y, Lemaire V, Zou G, et al. *Inorg. Chem.*, **2016,55**:5845-5852
- [18] Zhang Y R, Yu X, Jin Q H, et al. *Polyhedron*, **2017,138**:46-56
- [19] Yang J, Ma J F, Liu Y Y, et al. *Cryst. Growth Des.*, **2009,9**:1894-1911
- [20] Christopher J S, Michael J H. *Cryst. Growth Des.*, **2005,5**:1321-1324
- [21] Xiao Y H, Jin Q H, Deng Y H, et al. *Inorg. Chem. Commun.*, **2012,15**:146-150
- [22] Qiu Q M, Liu M, Jin Q H, et al. *J. Mol. Struct.*, **2014,1062**:125-132
- [23] Xu S, Liu M, Jin Q H, et al. *Polyhedron*, **2015,87**:293-301
- [24] Zhang L L, Zhong H, Zhao Y J. *Appl. Phys. Lett.*, **2009,94**:211106
- [25] SMART and SAINT, Siemens Analytical X-ray Instrument Inc., Madison: WI, **1996**.
- [26] Sheldrick G M. *SHELXS-97 and SHELXL-97*, Madison, WI, USA, **1997**.
- [27] Sheldrick G M. *SHELXTL NT Version 5.1*, University of Göttingen, Germany, **1997**.
- [28] Mathur T, Ray U, Baruri B, et al. *J. Coord. Chem.*, **2005,58**(5):399-407
- [29] Ruben D C, Daniel T, Jennifer A Z, et al. *J. Mater. Chem.*, **2011,21**(40):16108-16118
- [30] Li X L, Ai Y B, Shi Y H, et al. *Polyhedron*, **2012,35**:47-54
- [31] Xu X, Pooi B, Hong S H, et al. *Angew. Chem. Int. Ed.*, **2014,53**:1283-1287
- [32] Edwin C C, Catherine E H, Jennifer A Z, et al. *CrystEngComm*, **2011,13**:2742-2752
- [33] LIN Sen(林森), LI Yue(李跃), JIN Qing-Hua(金琼花), et al. *Chinese J. Inorg. Chem.*(无机化学学报), **2016,32**(12):2165-2171
- [34] Jin Q H, Yuan Y, Yang Y P, et al. *Polyhedron*, **2015,101**:56-64
- [35] Hiroki O, Atsushi K, Masako K. *Dalton Trans.*, **2014,43**:17317-17323
- [36] Coe B J, Fielden J, Foxon S P, et al. *J. Am. Chem. Soc.*, **2010,132**(10):3496-3513
- [37] Gahungu G, Zhang J. *Chem. Phys. Lett.*, **2005,410**(4/5/6):302-306